

THE SHALLOW STRUCTURE OF THE ROGGENPLAAT (THE NETHERLANDS) AS DEDUCED FROM HIGH-RESOLUTION MULTI-CHANNEL SEISMIC PROFILING¹

M. A. HERBER^{2,3}, D. J. RUNIA^{2,3} & K. HELBIG²

ABSTRACT

Herber, M. A., D. J. Runia & K. Helbig 1981 The shallow structure of the Roggenplaat (The Netherlands) as deduced from high-resolution multi-channel seismic profiling – Geol. Mijnbouw 60: 225-236.

High-resolution seismic profiling requires special instrumentation and special acquisition techniques, with a high-frequency source being the key factor. In a feasibility study on the Roggenplaat, a tidal flat in the mouth of the Oosterschelde (SW Netherlands), the CDP-method was applied using standard recording equipment together with a specially developed weight-drop unit. On areas with a high clay content results were obtained which were, in principle, good enough for a detailed investigation of the upper 120 m. However, due to the lack of well control in the area of investigation, only two major interfaces could be identified with some confidence.

The registration techniques used can be easily improved by using digital enhancement seismographs with digital recording on magnetic tape. However, the resolution obtained (about 2-3 m) can be repeated only in areas where the surface conditions are comparable to those of the survey area on the Roggenplaat: no weathered layer, high clay content, and a nearly complete water saturation.

INTRODUCTION

Diagnostic features of sedimentological interest often have typical dimensions of 0.1 to 100 m. Since two reflecting interfaces can be distinguished if their separation is larger than about a quarter of the dominant wavelength of the seismic signal (DOBRIK, 1976), seismic surveys directed at sedimentological targets must use signals with spectra centered at about 200 Hz (or more). Signals of such high frequency are not easily generated and are severely attenuated by surface layers that are either unconsolidated or reworked by biological and agricultural activities (the 'weathered layer'). Such surveys would thus have to be designed along the following lines.

(1) A high-frequency source buried beneath the weathered layer.

(2) High-frequency geophones buried beneath the weathered layer.

(3) A high-pass filter to suppress surface waves.

(4) Data processing capable of improving the signal-to-noise ratio without degrading the spectrum.

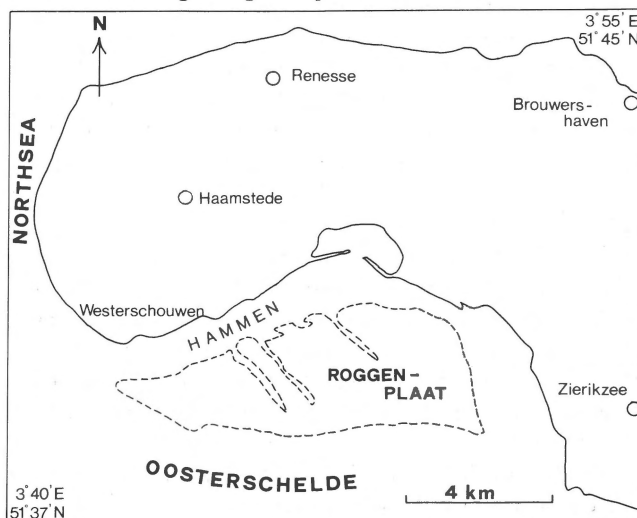


Fig. 1
Topographic map showing the location of the Roggenplaat.

¹ Manuscript received: 1981-02-05.

Revised manuscript received and accepted: 1981-04-02.

² Vening Meinesz Laboratory, Rijksuniversiteit Utrecht, P.O. Box 80.021, 3508 TA UTRECHT, The Netherlands.

³ Present address: Koninklijke Shell Exploration and Production Laboratory, Volmerlaan 6, 2288 GD RIJSWIJK, The Netherlands.

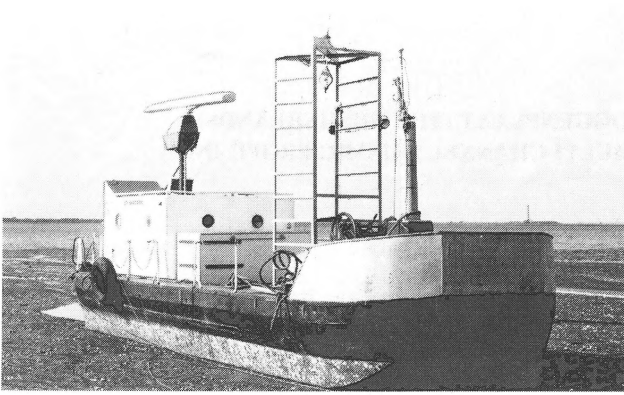


Fig. 2
Survey vessel of the MASE project group.

Closer analysis of these requirements reveals that they imply some further technical consequences: high-frequency sources are, by necessity, comparatively weak, so that the possibility to 'stack' (i.e. sum) data from repeated observations with the same acquisition geometry must be foreseen. Further, in the interest of improved signal-to-noise ratio and in order to obtain velocity information, common data point (CDP) technology should be applied. This requires data processing going beyond requirement (4) because, essentially, this can only be performed on digital computers, so that at some time during the processing, the data have to be available in digital form.

Today the problem of stacking and digitizing data and making them available for further processing is most easily solved with an enhancement seismograph with magnetic recording facilities. At the time of submission of this article, some of the data processing could have been done in the field using the above type of acquisition unit (Bison). However, in 1976, when this survey was started, most of this equipment did not yet exist. Moreover, at that time it was not at all clear whether the problems of signal generation and detection could be solved satisfactorily.

For this reason it was decided to carry out a feasibility study with equipment immediately available: a discarded 24-channel amplifier system and a set of geophones, both originally used in oil prospecting, and a 7-channel (analog) magnetic recorder. By a fortuitous set of circumstances the results were much better than expected.

The object for this study was suggested by the project group 'Modern and Ancient Sedimentological Environments' (MASE) of the Rijksuniversiteit Utrecht: the Roggenplaat, a tidal flat situated in the estuary of the Oosterschelde, south of the island of Schouwen-Duiveland in the South-West of The Netherlands (Fig. 1), and in particular the Holocene/Pleistocene boundary.

The logistic difficulties of operating on a tidal flat were by far outweighed by the advantages:

- (1) the absence of both vegetation and weathered layer;
- (2) only slight relief (10-50 cm);



Fig. 3
Weight dropping from the three-legged tower. The plate is submerged in the water. Foam-rubber cushions under the legs prevent the transmission of energy from the weight-release recoil into the ground.

- (3) the surface of the tidal flat is always water-saturated;
- (4) due to the remoteness of the area, noise caused by traffic and industry is virtually absent. The noise caused by natural forces was mainly due to wave action and observed only under certain weather conditions along the edges of the flat.

Work on a tidal flat requires the use of a boat to transport the equipment and the crew. This boat, made available by the MASE group, was beached shortly after high water at a predetermined point (Fig. 2). A crew of three then worked on the flat until the boat was re-floated by the returning tide.

The survey discussed in this paper was carried out during three field trips between december 1976 and july 1978.

DATA ACQUISITION

Source

All seismic observations were made using a falling weight as an energy source. A cylindrical or spherical weight of approx. 25 kg was dropped from a portable three-legged tower from a

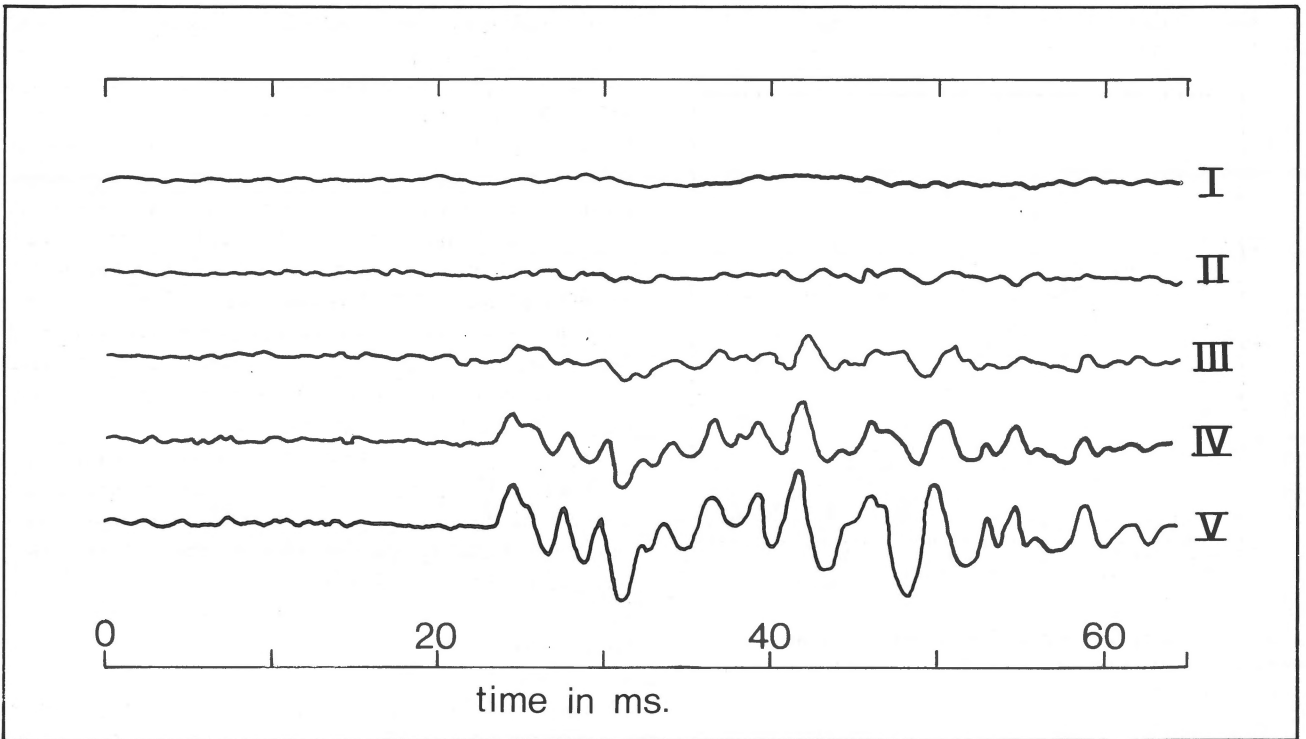


Fig. 4
Signal recorded at a distance of 44 m from the source for five individual drops of the weight. The striking increase of signal amplitude is due to the compaction of the ground under the base plate.

height of 2.5 m (Fig. 3). Foam-rubber cushions were placed under the legs of the tower to prevent transmission of the recoil (caused by the weight release) into the ground. The energy of the falling weight is partially converted into seismic energy on impact on the ground. The peak frequency of the signal is inversely proportional to the time between the impact and the moment the weight has zero velocity (the 'breaking time'). In order to reduce this time a circular baseplate with a diameter of 35 cm was used. The body waves produced in this way had a bandwidth of 200-300 Hz providing the required resolution. However, it should be mentioned that the 'breaking time' and thus the peak frequency depend strongly on the composition of the ground: in three different areas on the northern edge of the Roggenplaat, where the surface material is either clay with 10-20% sand or fine-grained sand, the peak frequency was well above 200 Hz. Observations on a fourth location on the Roggenplaat (Fig. 13), where the ground is composed of fine-grained high-porosity sand with some trapped air pockets (DE BOER, 1979), and on the beach of Schouwen-Duiveland (coarse high-porosity sand) resulted in peak frequencies of 100 Hz and 50 Hz, respectively. On pastures and agricultural roads in the Dutch polders the peak frequency is even lower.

The improvement of energy transmission with increasing compaction of the surface layer immediately below the base plate is illustrated by figure 4 showing records of five consecutive individual drops. Spectral analysis showed that the energy

increase occurred mainly in the frequency band between 200 and 280 Hz.

Detectors

The geophones were Hall-Sears type L1 with a natural frequency of 26 Hz and a damping of 0.65 of critical. These data

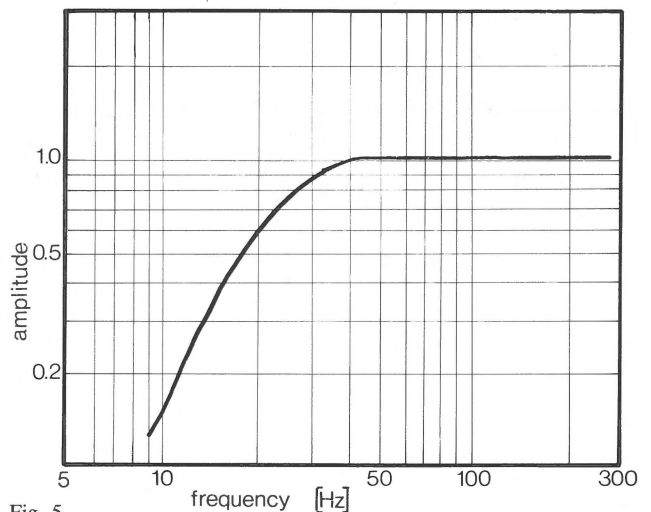


Fig. 5
Theoretical amplitude response curve of the HS L1 geophone used in the survey calculated with natural frequency $f_0=26$ Hz and $h=0.65$ of critical damping.

were checked in the lab before the geophones were taken to the field. Figures 5 and 6 show the theoretical response curves

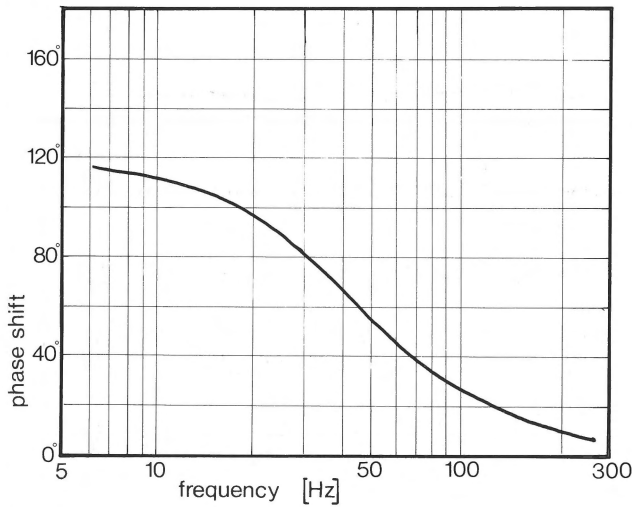


Fig. 6
Theoretical phase-response curve of the HS L1 geophone used in the survey calculated with natural frequency $f_0 = 26$ Hz and $h = 0.65$ of critical damping.

of the geophones (EVEN DEN ET AL., 1970). These curves seem to indicate that the geophones are at least equally suitable as geophones with a natural frequency of, say, 100 Hz, since the amplitude response is flat and phase shifts over the frequency band in question are smaller than for high-frequency geophones. Actually, this is not quite true: not only are the low-frequency surface waves (below 20 Hz) recorded about eight times as strongly as with 100 Hz geophones, but in actual response curves the 'clean pass band' is limited by spurious eigenfrequencies at about ten to twenty times the natural frequency. However, no serious difficulties were experienced due to the geophones: surface waves could be largely avoided due to the chosen acquisition geometry, and spurious eigenfrequencies were not evident in the data.

Single geophones –instead of the groups customary in standard surveys– were used since any array effective against long-period surface waves would have seriously degraded reflections from shallow interfaces at the oblique angles required by the acquisition geometry.

Field system

The complete field system used in the survey is shown in figure 7: a manually triggered pulse energizes the solenoid of the release armature so that the weight drops. On galvanic con-

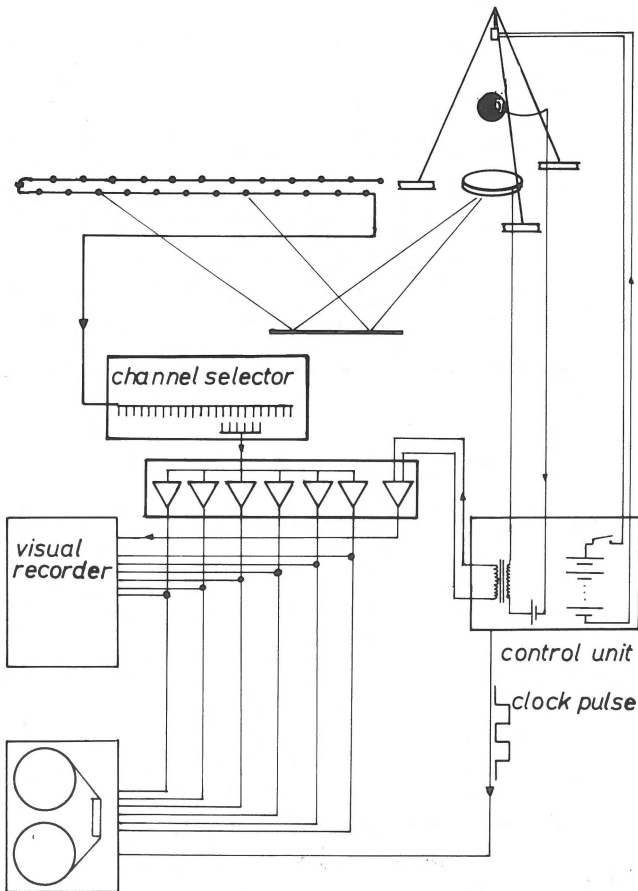


Fig. 7
Flow of signal and control in the seismic field system.

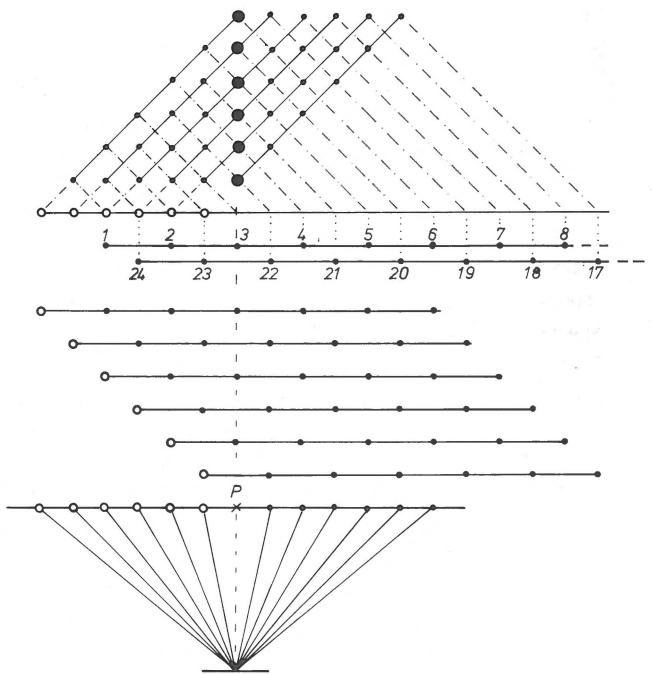
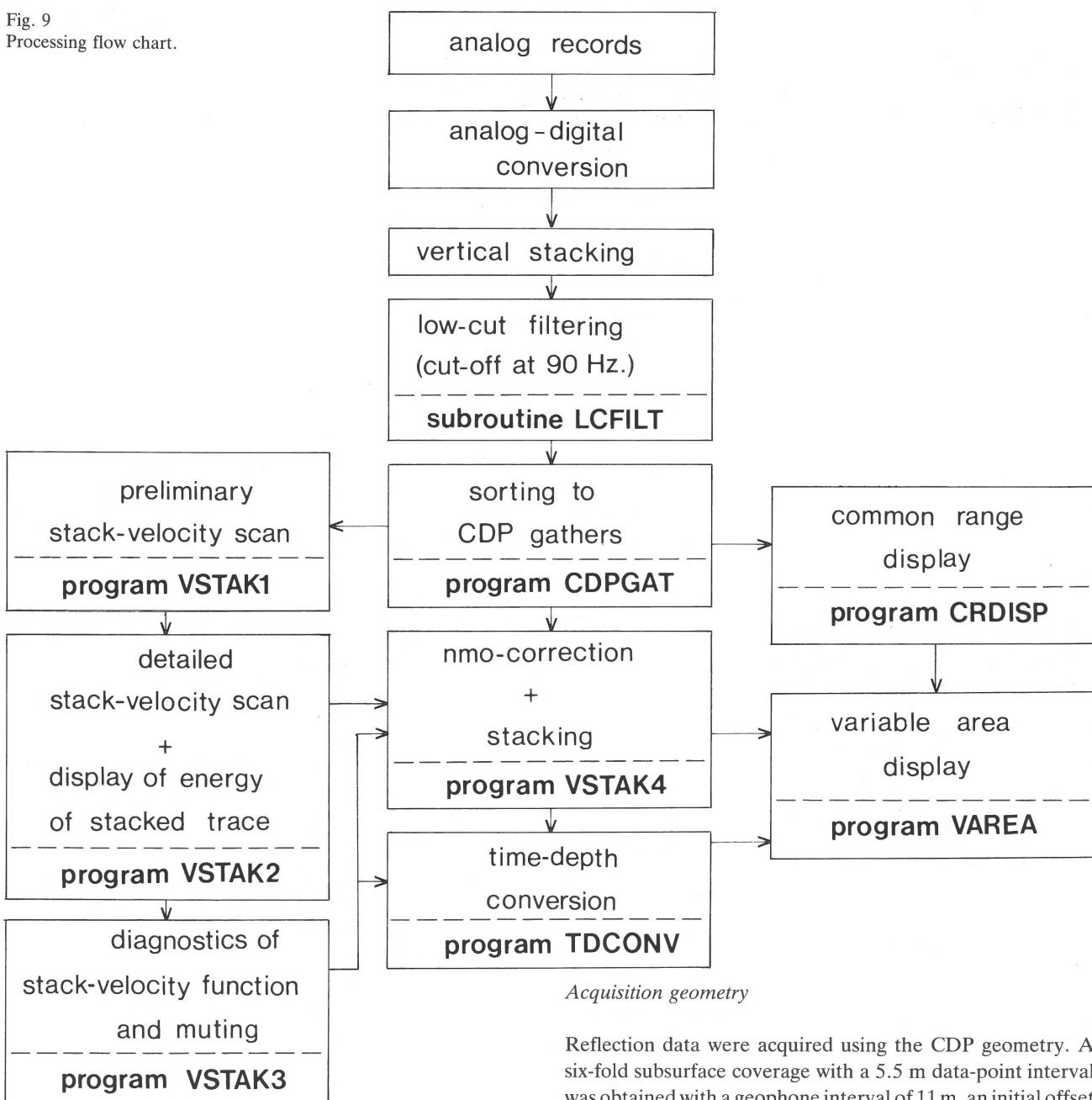


Fig. 8
CDP-gather centered at P and the source-geophone combinations used in its generation. In the upper part of the diagram each dot represents one source-receiver pair (sources: open circles). The 'data point' lies at the center of the pair and has the same coordinates as the dot in the diagram. Immediately below the diagram: geophone layout. Below: the six source-gathers that contribute to the CDP-gather centered at P.

Fig. 9
Processing flow chart.



Acquisition geometry

Reflection data were acquired using the CDP geometry. A six-fold subsurface coverage with a 5.5 m data-point interval was obtained with a geophone interval of 11 m, an initial offset of 11 m, and a source-point interval of 5.5 m. This geometry (Fig. 8) resulted in only one type of CDP gather.

DATA PROCESSING

Using the clock pulse on channel 7, the analog tapes were digitized on a 16-bit Raytheon 704 mini-computer and subsequently processed on the Cyber 73/28 computer of the Academic Computer Centre Utrecht. For this purpose a FORTRAN software package was developed. A flow chart of the subsequent processing steps is shown in figure 9.

In the 'vertical stacking' step, observations with identical

tact between weight and base plate a clock pulse (2000 Hz) is initiated that is recorded on channel 7 of the magnetic recorder. The signal from 6 (out of 24) geophones selected by the channel selector are amplified (constant gain: 90 dB in the 10-350 Hz frequency band) and recorded on channels 1 to 6 of the magnetic recorder. Visual monitor records can be taken with a direct recording camera on light-sensitive paper. During the survey this was done once for every weight-drop station.

Neither filters nor automatic volume control of the amplifier system were used, since none of the available settings was suitable for the times and frequencies encountered in the field.

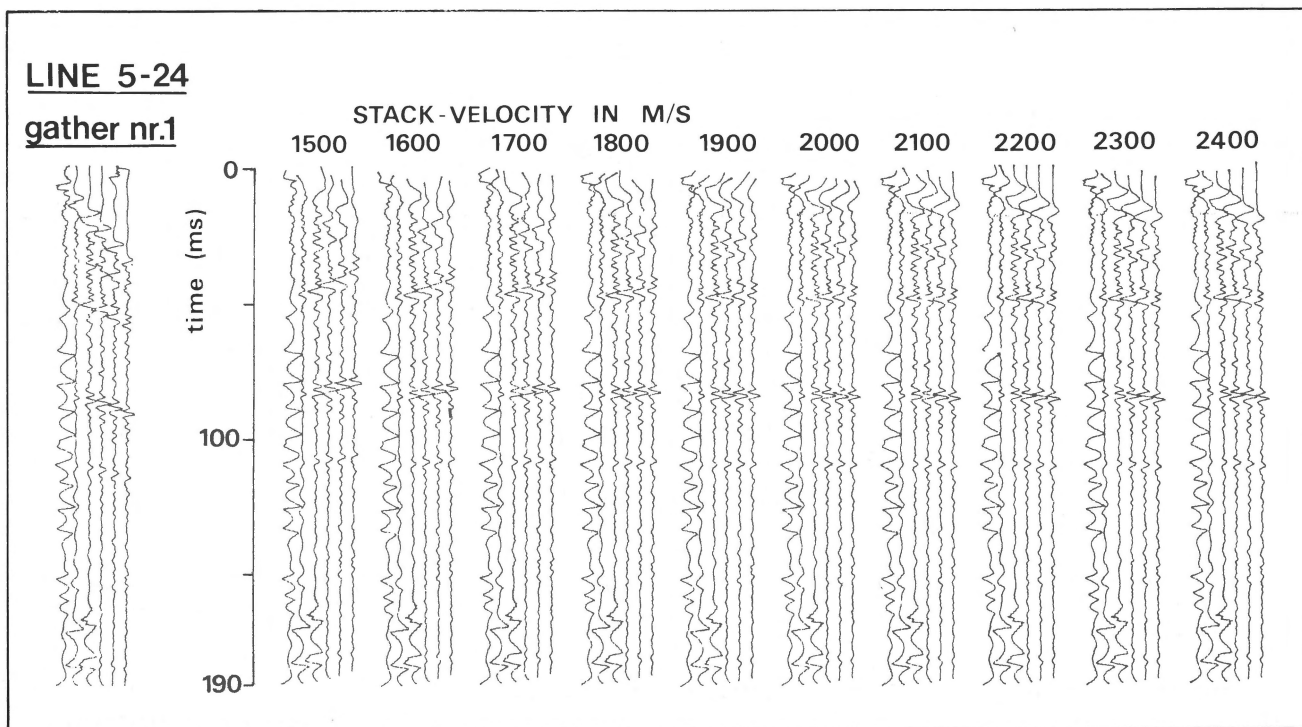


Fig. 10
Graphical output of program VSTAK1. Each panel has been corrected with a constant stack velocity. At correct velocity, arrival times become equal.

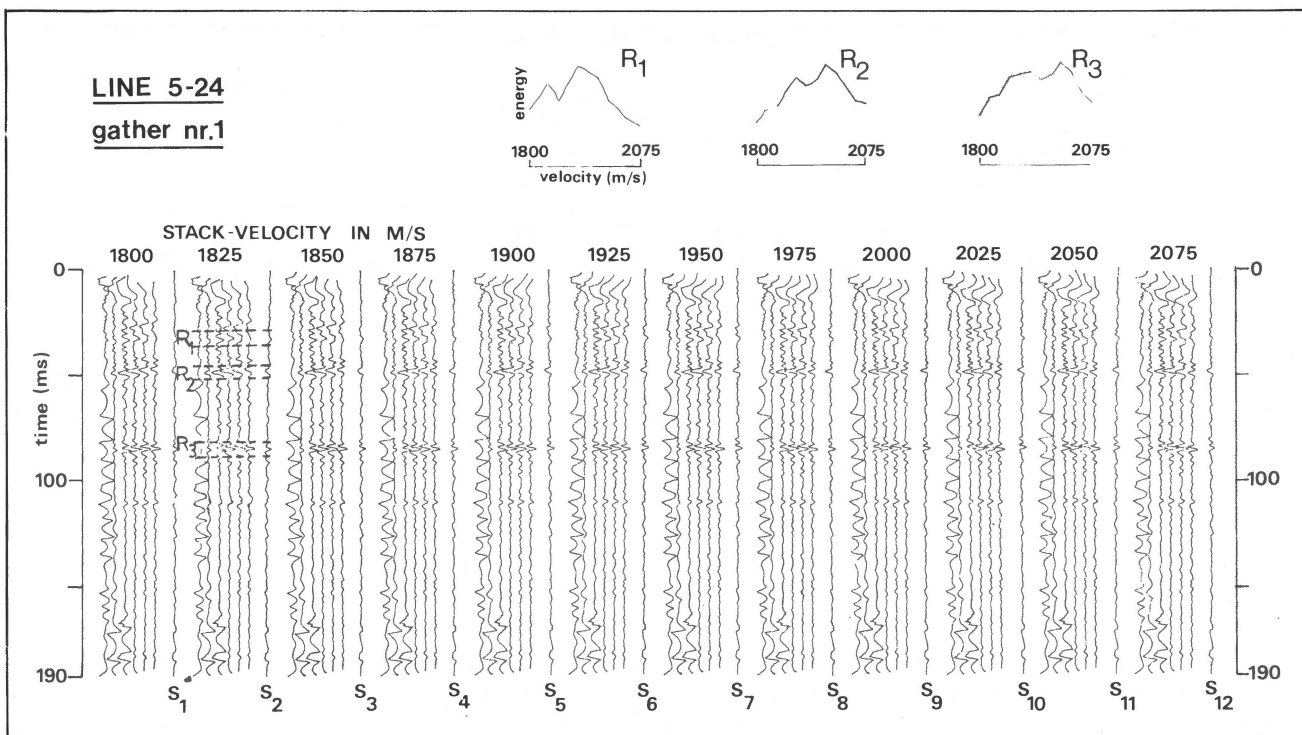


Fig. 11
Graphical output of program VSTAK2; panels corrected with velocities 1800-2075 m/s; S_1 - S_{12} : stacked traces; R_1 - R_3 line-ups for which stack energies have been calculated.

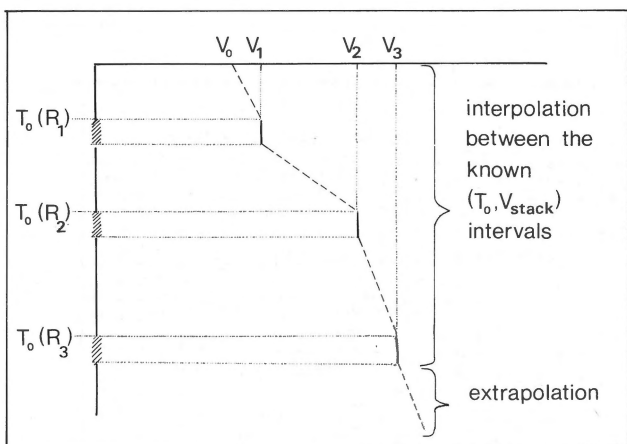


Fig. 12
Construction of stack-velocity functions by linear interpolation.

source and detector location are summed (4-fold) to improve the signal-to-noise ratio. Low-cut filtering for the elimination of surface waves is provided by subroutine LCFILT. For the current survey this turned out to be largely unnecessary: though the frequency ratio between signal and surface waves was large enough to permit a complete separation, surface waves arrived only on the two nearest channels during the time window of interest, but there the amplitudes were strong enough to be clipped, thus making any filtering impossible.

After sorting of the data into CDP-gathers (program CDPGAT) a velocity analysis was carried out in order to determine the optimum stacking velocities. In this process, the different arrival times within a CDP-gather—due to different source-detector separation—are corrected using a set of different velocities. This process is applied (program VSTAK1) to a number of CDP-gathers belonging to selected 'key'-data points in order to determine by visual inspection the velocity range where optimum stacking (i.e., horizontal line-up of reflections) occurs (Fig. 10). Within this range, program VSTAK2 repeats the process with smaller velocity increments. The total signal energy obtained after stacking serves as an indicator of the optimum stacking velocity at different arrival times (Fig. 11). From these data, a stack-velocity function is determined by linear interpolation (Fig. 12).

The actual stacking-after-correction of all CDP-gathers is carried out by program VSTAK4 using linear interpolations of the stack-velocity functions determined for the key mid-points. This program has optional facilities to suppress data that are degraded by first arrivals, clipping, or excessive data stretch on far-offset traces (of which the parameters were determined in VSTAK3). The stacked traces thus obtained are assembled to a time section and then displayed in variable area format as hard-copy section by program VAREA.

Two other types of hard-copy sections are provided: common-range displays and unmigrated depth-sections. In a common-range display, all traces have the same source-receiver separation ('range'). This largely obviates the corrections due

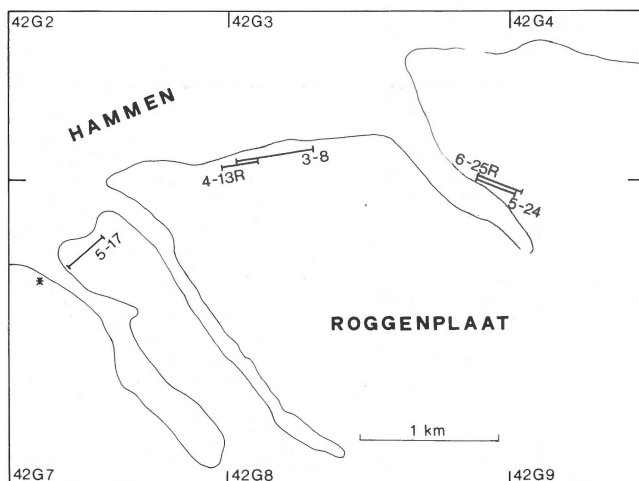


Fig. 13
Position of the seismic lines along the northern edge of the Roggenplaat; lines 5-17, 5-24 and 3-8 are reflection lines and 4-13R and 6-25R are refraction lines. At location x (left margin) low signal frequencies were observed. Coordinates adopted from Rijkswaterstaat.

to different travel paths. A common-range section thus can be used as preliminary information before the time-consuming stacking process. On the other hand, a common-range display indicates how data would have looked without CDP-stacking. In an unmigrated depth-section travel times are converted to distances using the stacking velocities. Slant rays—due to dipping reflectors or diffraction—are not taken into account in this display. Since only moderate dips were observed in this survey, this was regarded to be sufficient.

PROCESSING RESULTS AND REFLECTION MAPPING

Three reflection profiles were observed along the northern edge of the Roggenplaat (numbered 5-17, 3-8, and 5-24 on figure 13), together with two refraction lines for velocity control. Common-range sections, stacked time-sections, and unmigrated depth-sections were prepared for all three reflection profiles. Figures 14 and 15 show a common-range section and a time section of line 5-17. A comparison of these two displays shows strikingly the improvement in reflection continuity and in signal-to-noise ratio for reflection times greater than 20 ms that is afforded by CDP-stacking. The time sections of lines 5-24 and 3-8 are shown in figures 16 and 17. The three time sections show a wealth of structural detail for the travel time range between 15 ms and 140 ms (corresponding to a depth range of 15 to 145 m).

Reflection mapping and geological interpretation were based on the unmigrated depth-sections corresponding to these lines. For this mapping, all clear and strong phase line-ups were considered to be reflecting interfaces. The pulse produced by the falling weight was assumed to be a minimum delay pulse, and consequently the reflectors were positioned

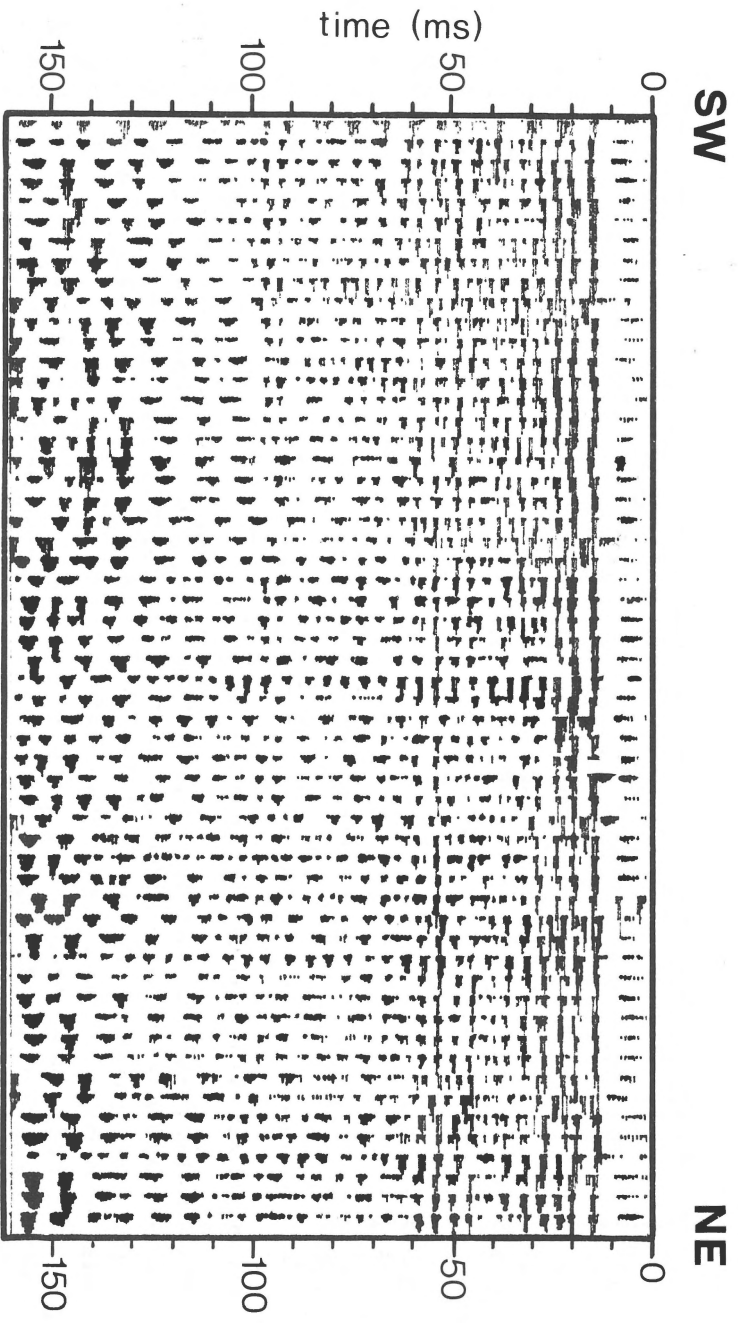


Fig. 14
Common-range display of line 5-17 for the range 22 m.

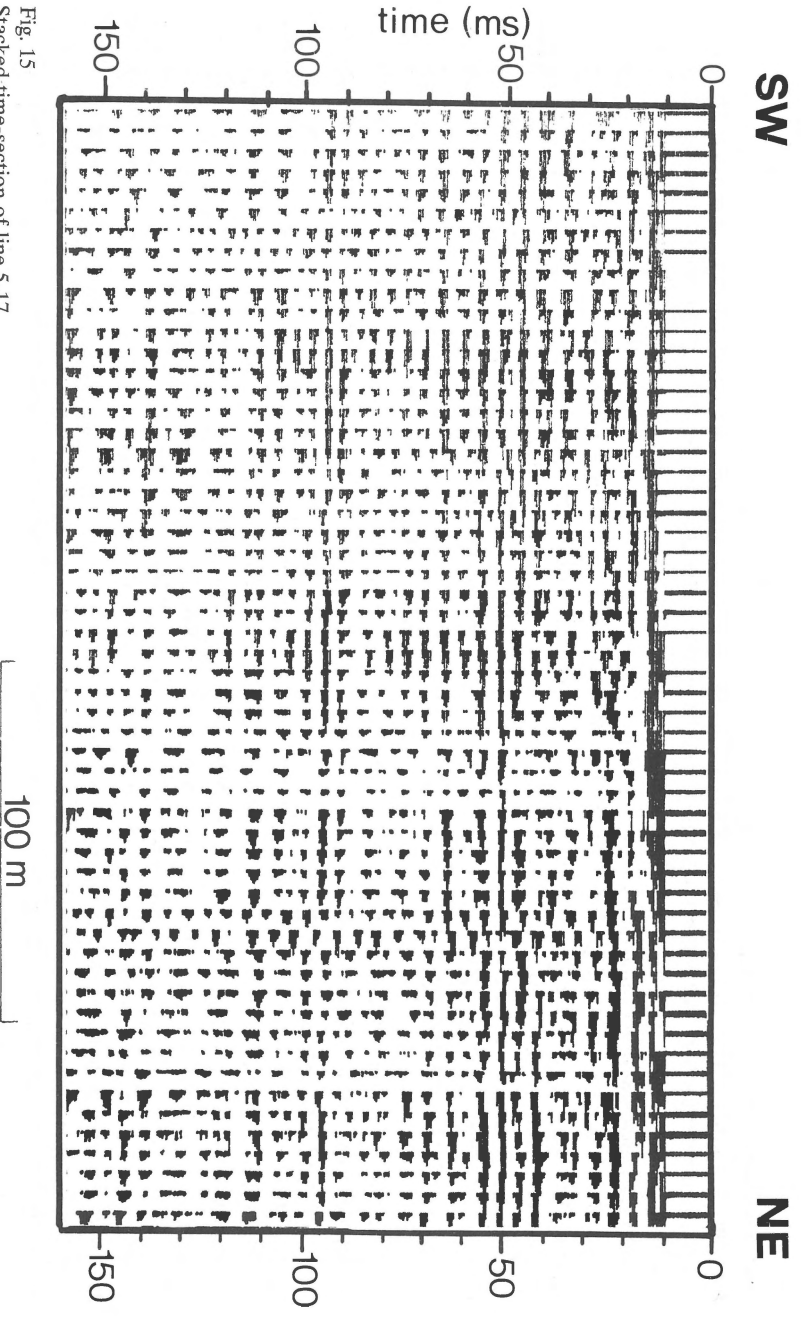


Fig. 15
Stacked time-section of line 5-17

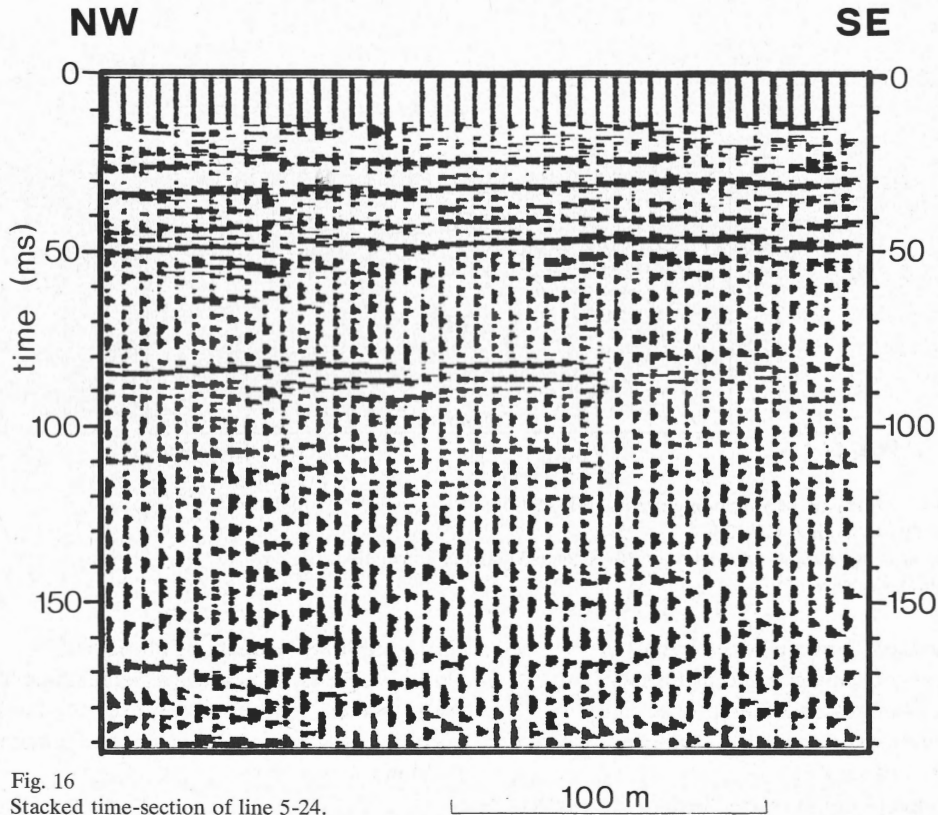


Fig. 16
Stacked time-section of line 5-24.

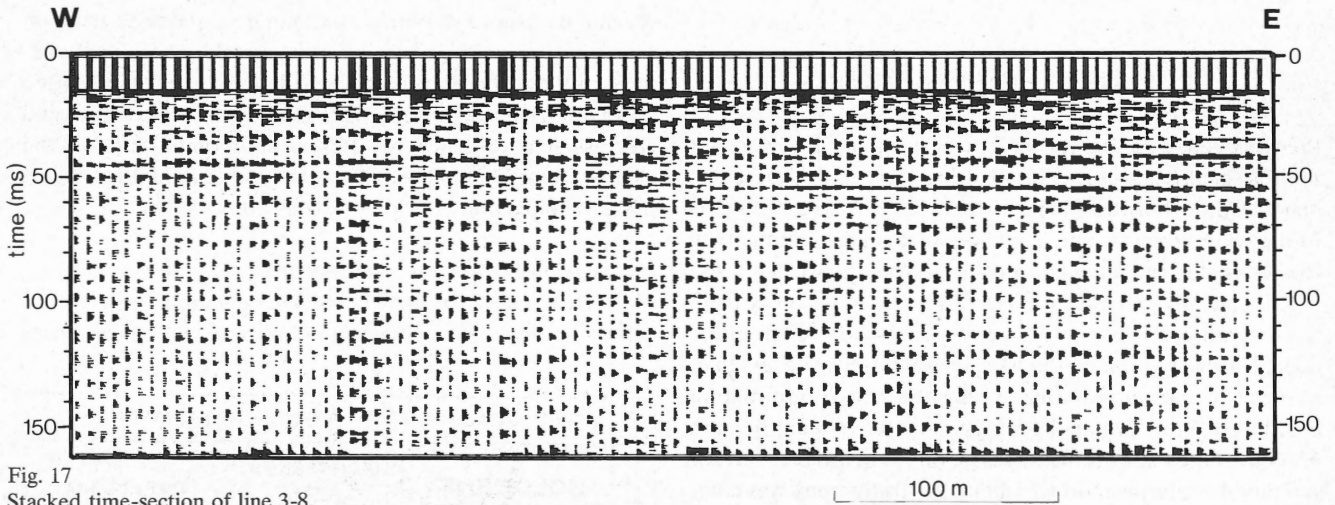


Fig. 17
Stacked time-section of line 3-8.

at the onset of the phase line-ups. Reflection picking was sometimes difficult, particularly with 'repetitive' signals that could represent either several reflections or a single reflection with a longer 'tail'. In such cases generally only the first line-up was accepted as a reflection.

The smallest detail in the time sections is of the order of 1.5-2 ms (corresponding to 1.5-2 m in the depth sections). This is in agreement with the generally assumed resolution of $T/4$ in seismic sections (DOBRIK, 1976). However, in view of the uncertainty of the correct positioning of 'repetitive' signals and the lack of information concerning the exact shape of the

pulse, the resolution and reliability of the interpreted depth sections of figure 18 might be only 3-4 m.

The interpreted depth sections of figure 18 have been divided into three zones. This division is based on seismic information only, namely:

- (1) reflection configuration (continuous, parallel, oblique etc.);
- (2) velocity information (e.g., a strong gradient in stacking velocities occurs at the boundary between zone I and II);
- (3) additional information from refraction observations (a strong refractor was found at a depth of about 40 m, thus

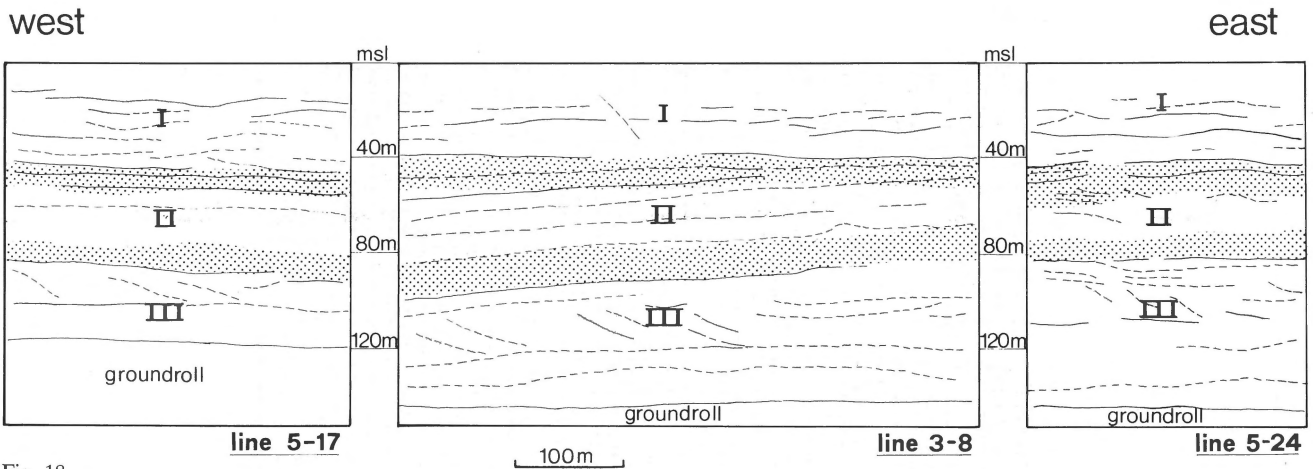


Fig. 18
Geological interpretation of tracings from unmigrated depth-sections.

Zone I: Holocene (Calais I - Duinkerke III).

Zone II: Miocene-Pleistocene (Breda, Oosterhout and Tegelen/Maassluis Formations).

Zone III: Oligocene and older (Rupel).

confirming the boundary between zones I and II).

The zones can thus be characterized as follows:

Zone I: many discontinuous undulating reflections;

Zone II: parallel reflections, slightly dipping. Velocities markedly higher than in zone I;

Zone III: parallel reflections intermixed with oblique reflections with a general apparent dip towards the east.

GEOLOGICAL INTERPRETATION

Precise deeper geological information on the Roggenplaat itself is scant (FERMONT, 1976). During the past few decades, many shallow borings (TD less than 120 m) have been performed on Schouwen-Duiveland as well as in the mouth of the Oosterschelde (in connection with the Deltaplan), but these borings are without exception several kilometres away from the Roggenplaat. Recently four very shallow boreholes (less than 35 m) were sunk on the Roggenplaat itself, one less than a km from our survey area. Using the above information together with the regional geology, a tentative identification of some of the major reflectors is possible. In order to further simplify the interpretation a schematic stratigraphy was compiled (VAN RUMMELLEN, 1970 ; ZAGWIJN & VAN STAALDUINEN, 1975), for the depth range from sea level to 140 m below sea level, corresponding to a geological section from Upper Oligocene to the present-day sediments of the Holocene (Fig. 19).

(1) Rupel Formation (Boomse klei), Upper Oligocene. This formation consists of a dense, marine clay deposited presumably on tidal flats (thickness > 60 m).

(2) Breda Formation, Middle Miocene.

This formation consists of marine, clayey, glauconite containing sands, fine to very fine-grained (thickness 10-20 m).

(3) Oosterhout Formation, Pliocene.

Marine deposits, consisting of medium fine to medium coarse grained sands. Shell fragments are abundantly present, often in layers and sometimes cemented in isolated beds (thickness 15-20 m).

(4) Maassluis Formation, Pleistocene.

Marine nearshore deposits, containing very fine to medium fine sands, intercalated with clay layers of up to 0.5 m thickness. Isolated beds of cemented shell fragments are often observed. After deposition these sediments were dehydrated (regression); evidence for this is a limonite skin on the foraminifera. Due to this dehydration these sediments have a higher compaction (thickness variable).

(5) Tegelen Formation, Pleistocene.

Fluvial equivalent of the Maassluis Formation consisting of carbonate-free sands. Numerous clay intercalations as lenses

		TIME SCALE	LITHOSTRATIGRAPHY
quaternary	HOLOCENE		DUINKERKE FM. CALAIS FM.
		TIGLIEN interglacial	TEGELEN FM.
	PLEISTOCENE	PRAETIGLIEN glacial	MAASSLUIS FM.
tertiary	PLIOCENE		OOSTERHOUT FM.
	MIOCENE		BREDA FM.
	OLIGOCENE		RUPEL FM.

Fig. 19

Schematic stratigraphical column for the Roggenplaat.

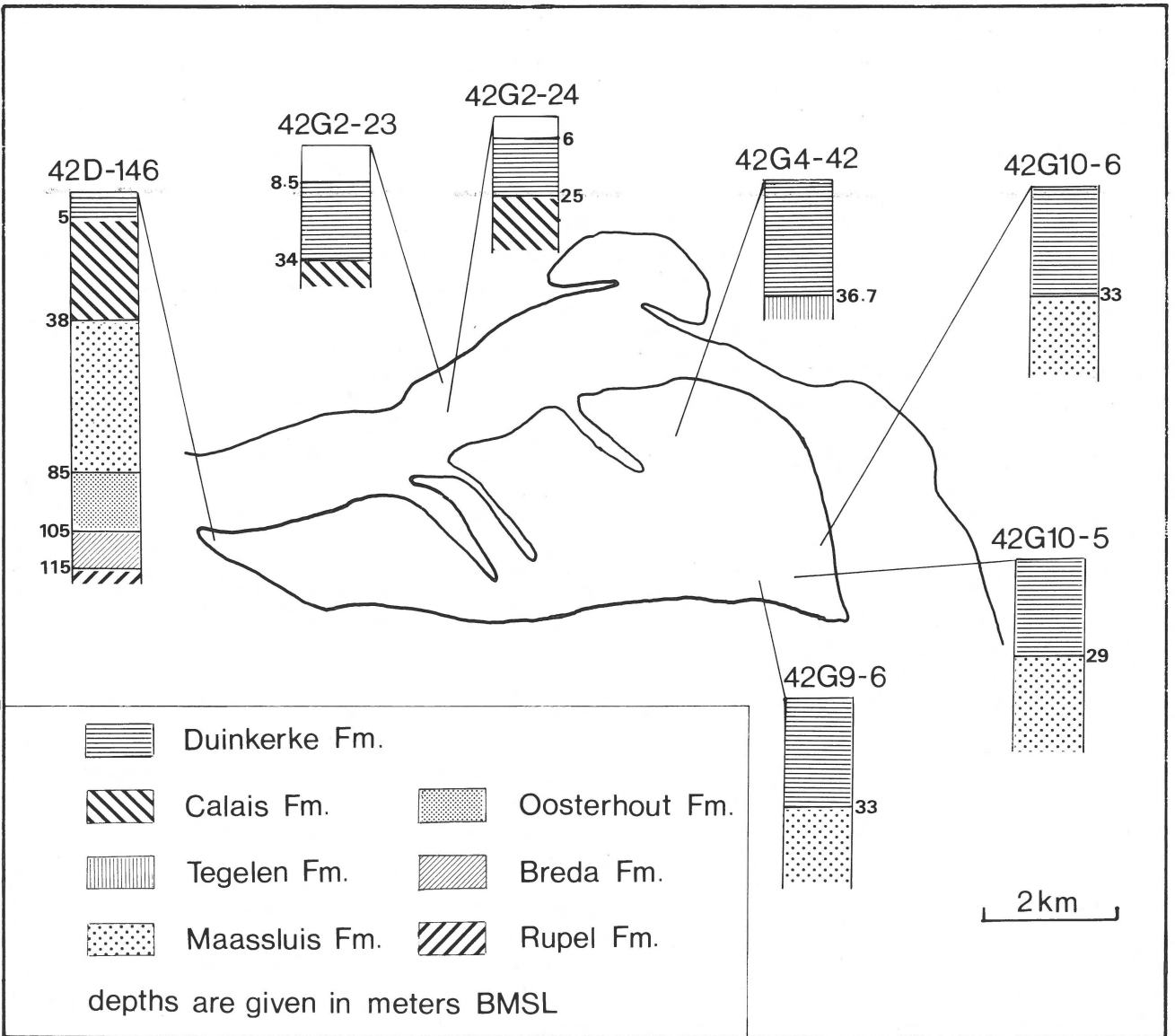


Fig. 20
Location and results of borings on the Roggenplaat and in the immediate vicinity.

and as layers with a thickness of several metres. These sediments have also been dehydrated over a certain period after deposition, which resulted in a strong compaction. The deposits belong to a system of fluvial channels which eroded in the marine sands of the Maassluis Formation. The general trend of these channels is N-S (thickness variable).

(6) Calais Formation, Holocene.

Marine clayey sands with many clay layers of several metres thickness. These sediments were deposited in tidal channels and on tidal flats during various transgressive phases (Calais I-IV). Inbetween these phases fluvial channels eroded in the marine sands indicating phases of regression. Both transgressive and regressive channel systems often eroded into the underlying Tegelen Formation and sometimes even through

the Tegelen Formation into the deeper lying Maassluis Formation (thickness variable).

(7) Duinkerke Formation, Holocene.

Marine clayey sands with intercalations of clay layers (< 0.5 m) deposited as channel-fills of several subsequent transgressive channel systems (Duinkerke 0-III). These channel systems eroded into the Calais Formation as well as into the Tegelen Formation (the channels reach a maximum depth of 40 m).

It is obvious that in the Pleistocene/Holocene timespan, complicated stratigraphic patterns were formed due to the subsequent erosional channel systems of both tidal (transgressive) and fluvial (regressive) nature. Especially in the Holocene

several phases of transgression can be discerned.

The last influential eroding channel is what we now call the 'Hammen' (Fig. 1) which migrated northwards during the last centuries. The sediments which were deposited after the passing of this channel are grouped under the name Duinkerke III. Because the maximum depth of the Hammen in recent geological time is not exactly known, there are several possibilities for the stratigraphy on the Roggenplaat which can have a very local character.

Duinkerke III can have been deposited (with erosive contact):

(1) directly on the Pleistocene formations (Tegelen or Maassluis) which is seen in boring 42G4-42 (Tegelen) and in borings 42G9-6, 42G10-5 and 42G10-6 (Maassluis). The locations of these borings are marked in figure 20;

(2) on the Calais Formation which in turn has eroded into the Pleistocene, as was found in borings 42G2-23 and 42G2-24;

(3) on earlier Duinkerke 0, I and/or II (formed by 'pre-Hammen' channel systems) which in turn have the same possibilities as Duinkerke III in (1) and (2). This would be the case if the Hammen had (locally) been shallow and therefore not have eroded deeply into the Duinkerke I and II deposits.

The occurrence of those possibilities is shown in figure 20 in which all drilling information is schematically drawn. From this figure and the foregoing discussion we see that not enough information is available at present to form a clear picture of the geological structure of the Roggenplaat.

The geological setting outlined above allows some a priori remarks concerning the interpretation of the seismic sections.

(1) It is unlikely that any of the seismic reflectors in zone I can be unambiguously related to a specific formation or member of the Holocene (Calais I-IV and Duinkerke III).

(2) The upper boundary of the Pleistocene Tegelen and/or Maassluis Formations should be detectable. The reason for this is threefold.

(i) Due to the dehydration of the Pleistocene and the resulting compaction the Pleistocene/Holocene boundary is likely to mark a significant velocity and impedance contrast.

(ii) In boring 42G4-42 the upper boundary of the Pleistocene (Tegelen) was reached at 36.70 m, where it consists of a dense clay layer. The overlying Holocene (Duinkerke III) consists of clayey sand. Reflection line 5-24 lies only a few hundred metres from the boring.

(iii) Both refraction lines show a strong refractor at about 40 m depth.

(3) The only pre-Pleistocene interface that can be identified with some confidence is the boundary between the Breda Formation and the Rupel Formation. The impedance contrast at this boundary is due to the juxtaposition of clayey sands (Breda) and very dense clay (Rupel). We identify this boundary with a strong reflector at about 95 m (see also boring 42G-146 at the mouth of the Oosterschelde, Fig. 20).

These considerations lead to the geological identification of the zones in figure 18. It is stressed that this interpretation remains tentative as long as no deep boring is sunk on the Roggenplaat itself.

CONCLUSIONS

In spite of the improvised nature of the equipment used, the results are surprisingly good. The high quality of the data is due mainly to two contributing facts: the high frequency of the signals generated by an impact on the surface in the survey area and the significant improvement due to the CDP-technology. It is likely that an extension of the survey with more modern equipment will yield even better results (to say nothing of the operational simplification to be expected from immediate stacking and digitization). It is unfortunate that one of these two factors—the high signal frequency—does not automatically apply to other survey areas.

Though the sections contain a multitude of distinct reflections, only two could be identified with geological boundaries with some confidence. Many more—and more reliable—identifications are to be expected from a seismic line in the immediate vicinity of a borehole.

ACKNOWLEDGEMENTS

This article is based on the 'doctoraal thesis' of two of us (M.A.H. and D.J.R.). We wish to thank all those who helped during the survey: Nio Swie Djin and the MASE project group for the use of their boat and for many small things that were indispensable in our work; Johan Tempels for help in developing equipment; H. Innemee for help in the field; and the teaching staff of the Vening Meinesz Laboratory for general assistance with theoretical, experimental, and logistic problems.

REFERENCES

- De Boer, P. L. 1979 Convolute lamination in modern sands of the Oosterschelde estuary, The Netherlands, as the result of entrapped air – *Sedimentology* 26: 283-294.
- Dobrin, M.B. 1976 Introduction to geophysical prospecting (3rd ed.) – McGraw-Hill (New York).
- Evenden, B.S., D.R. Stone & N.A. Anstey 1970 Seismic prospecting instruments, Volume 2 – *Geoexplor. Monogr.* 1, Borntraeger (Stuttgart).
- Fermont, W. 1967, Paleogeografische ontwikkeling van de Roggenplaat – MASE rept. 4, Inst. Earth Sci. Utrecht.
- Van Rummelen, F.F.F.E. 1970 Toelichtingen bij de geologische kaart van Nederland 1:50 000, Blad Schouwen-Duiveland – Rijks Geol. Dienst (Haarlem).
- Zagwijn, W.H. & C.J. van Staalduinen (eds.) 1975 Toelichtingen bij de geologische overzichtskaart van Nederland 1:600 000 – Rijks Geol. Dienst (Haarlem).